

Ke Ren and Haiyang Gao
School of Atmospheric Physics
Nanjing University of Information
Science and Technology
Nanjing, 210044, P. R. China
E-mail: renke0412@gmail.com

June 10th, 2024

Re: Manuscript Number: AMT-2023-186

Title: Simulation and detection efficiency analysis for polar mesospheric clouds measurements using a spaceborne wide field of view ultraviolet imager

Author: Ke Ren; Haiyang Gao; Shuqi Niu; Shaoyang Sun; Leilei Kou; Yanqing Xie; Liguang Zhang; and Lingbing Bu

Dear Reviewer,

Thank you for your review of the manuscript entitled “Simulation and detection efficiency analysis for polar mesospheric clouds measurements using a spaceborne wide field of view ultraviolet imager” pending revision as well as for your valuable suggestions to improve the paper. We have tried every means possible to improve the presentation and increased the readability. We have also made all the changes suggested by the reviewer and addressed all the comments in the notes below. Please note that the reviewer’s comments are shown in bold type and our responses in plain type.

Best regard,

Ke Ren and Haiyang Gao

GENERAL COMMENTS:

This paper presents an analysis of anticipated performance for a wide field-of-view ultraviolet imager (WFUI) instrument designed to observe polar mesospheric clouds (PMCs). The WFUI is based on the Cloud Imaging and Particle Size (CIPS) instrument flown on the Aeronomy of Ice in the Mesosphere (AIM) satellite, but with only one forward-looking camera instead of four cameras. A database of expected PMC behavior and the For Ice Experiment (SOFIE) instruments. This database is used in a forward model to simulate the performance of the WFUI for a wide range of conditions. The likelihood of successfully detecting a PMC is shown to be dependent on ice water content, which has implications for the results available at different latitudes and different times during a PMC season.

The paper is well-written and comprehensive. Selected comments are listed below.

SPECIFIC COMMENTS

1. Page 3, lines 75-76: I would clarify this statement to say that CIPS is the only nadir view instrument to use multiple views of the same location and phase function effects to identify PMCs. SBUV-type instruments also use nadir viewing and UV wavelengths, but with only one large pixel.

Thanks for the reviewer's good comment. We appreciate your clarification, and we have modified this sentence (lines 75-76) as:

"...CIPS is the only nadir view instrument to use multiple views of the same location and phase function effects to identify PMCs. SBUV-type instruments also use nadir viewing and UV wavelengths, but with only one large pixel..."

2. Page 4, lines 100-101: This operating concept sounds similar to CIPS, except that CIPS uses 4 cameras (forward, backward, left side, right side) to get multiple views of each location at different scattering angles (SCA). The large variation in phase function with SCA for small ice particles then enables identification of pixels containing PMCs. Since the WFUI instrument will only capture 1 (or perhaps 2) images of a given location with much less SCA variation, how will PMCs be identified relative to the background signal?

Thanks for pointing this out. We have discussed this issue, and the information has been incorporated.

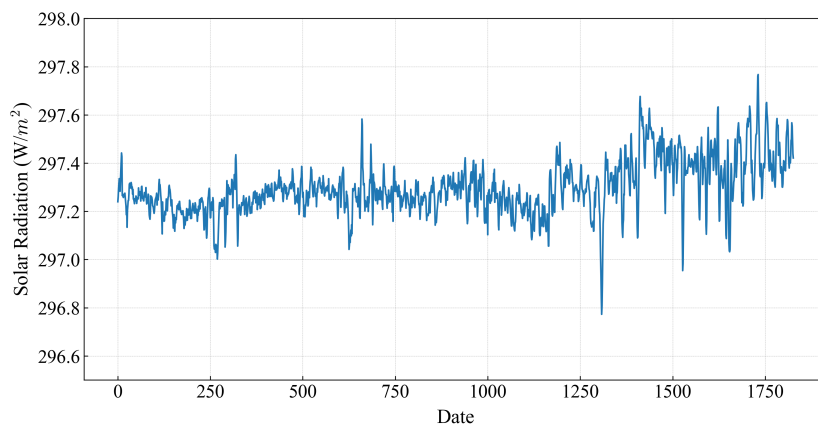
As mentioned by the reviewer, CIPS has four cameras, which gives it the ability to detect weak PMCs by examining the phase function from SCA with significant differences. However, by an intermittent exposure, the WFUI instrument can capture two (or more) images of a given location, but with a scattering angles (SCA) variation of only 20-40 degrees. This indeed makes it challenging to identify weaker PMCs, which is one of the reasons for the lower detection efficiency in regions of weaker PMCs. However, using a single camera significantly reduces costs and minimizes payload space. Also, WFUI is potential to be installed on multiple CubeSats to detect the same sampling PMCs region with variation scattering angle when different CubeSats are orbiting in the same orbit with a certain delay time interval. This would allow obtaining multiple views of each position from different SCA, thereby improving the detection of weaker PMCs.

Thus, we added some description to Section 4.4 (line 496 to 500) as:

“...WFUI with only one camera cannot achieve the level of CIPS with four cameras when detecting small particles in weak PMCs. However, using a single camera significantly reduces costs and minimizes payload space. Also, WFUI is potential to be installed on multiple CubeSats to detect the same sampling PMCs region with variation scattering angle when different CubeSats are orbiting in the same orbit with a certain delay time interval. This would allow obtaining multiple views of each position from different SCA, thereby improving the detection of weaker PMCs. ...”

3. Page 7, lines 171-173: Why not use an observed solar reference spectrum? One example is the TSIS-1 Hybrid Solar Reference Spectrum (HSRS), available at the LASP Solar Irradiance Datacenter (<https://lasp.colorado.edu/lisird/>).

Thanks for the reviewer's good comment and instruction. We downloaded the daily average solar spectrum data from “https://lasp.colorado.edu/lisird/data/gsfsc_composite_ssi” to recalculate the simulation result. This dataset covers the wavelength range of 120.5-499.5 nm in 1 nm bins, spanning from November 8, 1978, to July 24, 2022. It was generated by merging public irradiance data from nine satellite instruments: SME, Nimbus-7 SBUV, NOAA-9 SBUV/2, NOAA-11 SBUV/2, UARS SUSIM, UARS SOLSTICE, NOAA-16 SBUV/2, Aura OMI, and SORCE SOLSTICE. The daily variation of ultraviolet solar radiation from 2008 to 2012 is shown in the following figure.



After recalculation, we have updated Figures 6 to 9. Since the solar radiation calculated by using the Planck equation does not account for atmospheric absorption, the calculated value of solar radiation is higher than the actual reference spectrum. Therefore, the recalculated simulation signal has decreased after recalculation, as can be seen from Figures 6 and 7. However, this adjustment has a minimal impact on detection efficiency. The recalculated detection efficiency of the example orbit decreased from 81.64% to 81.09%. Figures 8 to 9 show slight changes, while the overall trend remains unchanged. The formula (19) for fitting the correlation curve between detection efficiency and IWC from 2008 to 2012 has been revised.

Thus, we have modified the sentence (lines 181 to 184) as:

“... The WFUI was designed as a UV camera, so we utilized observed daily average solar UV spectral data to calculate solar radiation. This data can be acquired from the LASP Solar Irradiance Data Center (<https://lasp.Colorado.edu/Liird/>). The dataset covers the wavelength range of 120.5-499.5 nm in 1 nm bins, spanning from November 8, 1978, to July 24, 2022. It

was generated by merging public irradiance data from nine satellite instruments. ...”

We have modified the eq. 6 (line 187-188) as:

$$S = \sum_{\lambda=\lambda_2}^{\lambda=\lambda_1} (E_{\lambda} \times t_{\lambda}) = \sum_{\lambda=\lambda_2}^{\lambda=\lambda_1} \left(E_{\lambda} \times \frac{t_{fmax}}{1 + \left[\frac{2(\lambda-\lambda_0)}{FWHM} + \frac{\lambda}{FWHM} \frac{\theta_0^2}{n_e^2} \right]^2} \right) \quad (6) \quad ”$$

“... where E_{λ} is daily average solar spectra ...”

We have modified the sentence (line 391) as:

“... the detection efficiency of PMCs by the WFUI was determined to be 81.09 % ...”

We have modified the eq. 19 (line 434) as:

$$\eta_d = -2.211 \times e^{\frac{IWC}{86.580 + 1.299}} \quad (19) \quad ”$$

The updated Figures 6 to 9 and the captions are modified as follows:

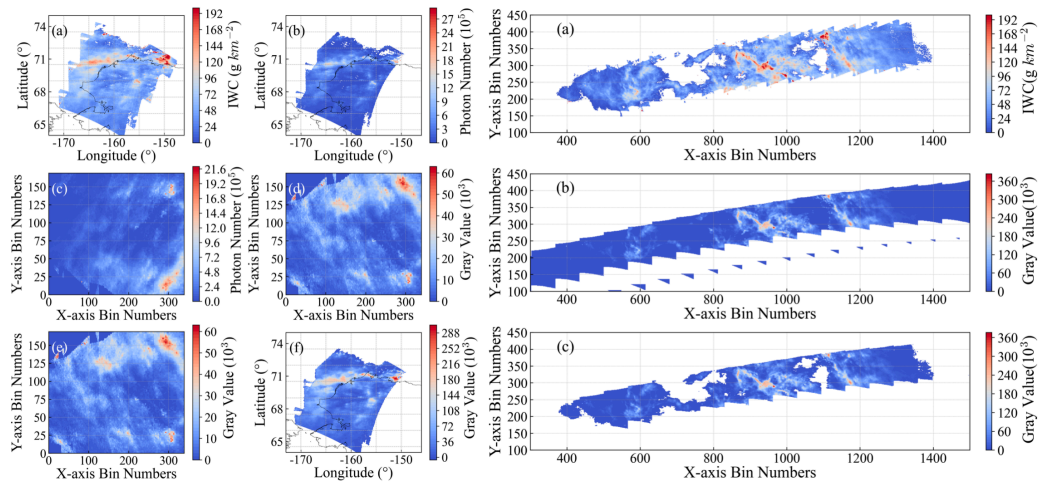


Figure 6: (a) Distribution of IWC with latitude and longitude for a single image detected by CIPS. (b) Distribution of the Photon number with latitude and longitude for a single image detected by WFUI. (c) IWC of the orbit detected by CIPS. (d) Photon number corresponding to the single image pixels. (e) Gray value corresponding to the single image pixels. (f) The gray value of the orbit detected by WFUI. (g) Gray value of the single image after the denoising process. (h) Distribution of gray value with latitude and longitude for the single image after the denoising process. (i) Gray value of the orbit after the denoising process of WFUI.

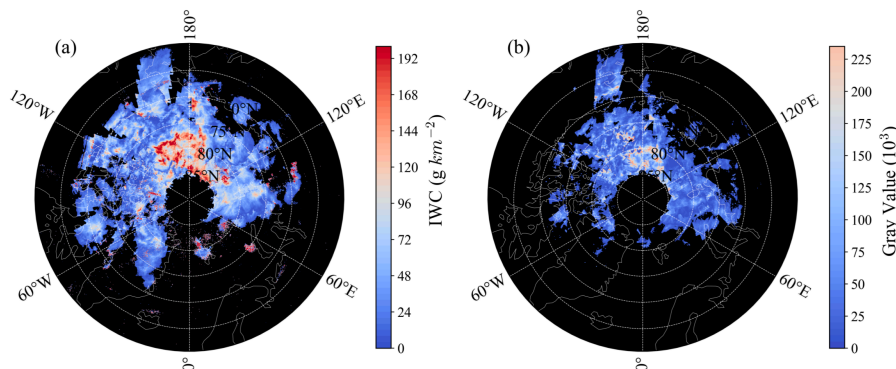


Figure 7: (a) Distribution of IWC on August 3, 2011, detected by CIPS. (b) Simulating distribution of gray value.

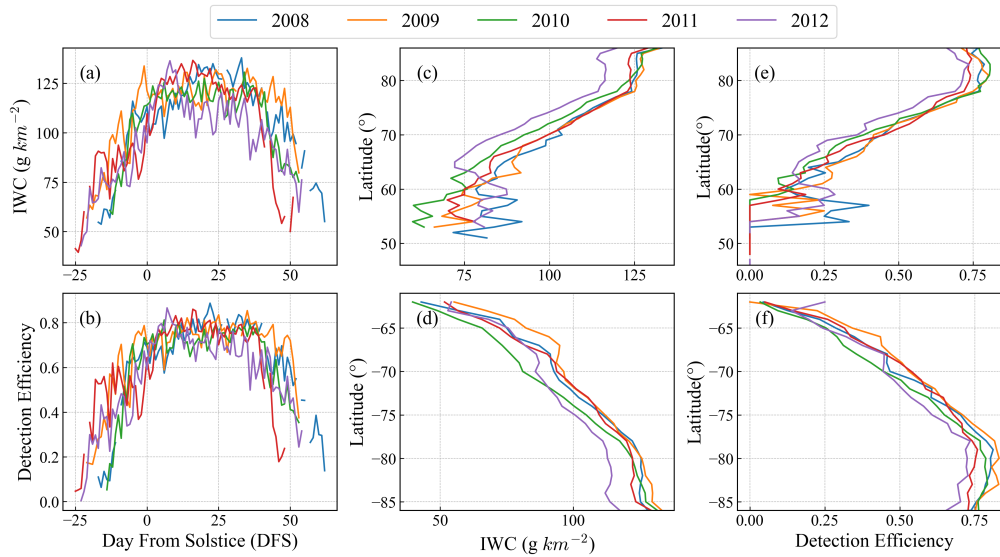


Figure 8: (a) Average daily variation of IWC in PMCs season from 2008 to 2012. (b) Average daily variation of detection efficiency in PMCs season. (c) Variation of IWC with latitude in the northern hemisphere during the PMCs season from 2008 to 2012. (d) Variation of IWC with latitude in the southern hemisphere. (e) Variation of detection efficiency with latitude in the northern hemisphere. (f) Variation of detection efficiency with latitude in the southern hemisphere.

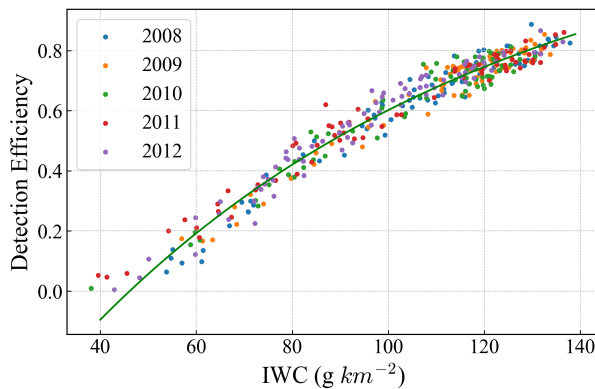


Figure 9: Correlation between the IWC and detection efficiency in the PMCs season for both hemispheres.

4. Page 8, line 188: An optical thickness as large as 3 seems very high for a PMC, particularly in nadir viewing geometry. A recent paper by Lubken et al. [2024] (<https://doi.org/10.1029/2023GL107334>) gives a mean optical depth for PMCs of $\sim 0.04-0.05$ at 126 nm and 69 degrees N latitude for the year 2020.

Thanks for the reviewer's suggestion. The optical thickness of PMCs has been adjusted to 0-0.3. We appreciate the reference you mentioned which is extremely helpful, and we have modified the sentences (lines 196-198) as:

"...The optical thickness of PMCs is usually 0–0.3, which is consistent with the approximation of single scattering calculations. Generally, mean optical depth of PMCs from observation can be $\sim 0.04-0.05$, and the maximum value can reach 0.2-0.3 (Lubken et al., 2024) ..."

We have added this reference to the end:

“Lubken, F. J., Baumgarten, G., Grygalashvyly, M., and Vellalassery, A.: Absorption of solar radiation by noctilucent clouds in a changing climate, Geophys. Res. Lett., 51(8), e2023GL107334, <https://doi.org/10.1029/2023GL107334>, 2024.”

5. Page 16, lines 371-373: This statement sounds like you will subtract a calculated noise term and assume that a positive residual signal represents a PMC detection. But the total observed signal also contains a background component determined by the amount of stratospheric ozone, which varies with time and latitude. Fluctuations in ozone could lead to false detections in your algorithm. Can you discuss how you would address this concern?

Thanks for pointing this out. We have added several references and discussed this concern of the reviewer.

The satellite data indicate that total ozone varies strongly with latitude over the globe, with the largest values occurring at middle and high latitudes during most of the year. In the Antarctic, a pronounced minimum in total ozone is observed during spring. Typical values vary between 200 and 500 Dobson units (DU) over the globe, with a global average abundance of about 300 DU (Salawitch et al., 2023). Calculations show that even lower concentrations of ozone can effectively absorb solar UV radiation, preventing UV radiation from below altitudes of 40 km, which is scattered by the ground, lower atmosphere, and cloud/aerosol layer, from being uploaded.

Studies have found that after the AIM satellite's orbit was lowered, it could detect Rayleigh scattering of 265 nm radiation at altitudes around 50-55 km when there were no PMCs. Coherent perturbations to the observed Rayleigh scattering signal on scales of tens to hundreds of kilometers generally indicate GW-induced variations in the neutral density and/or ozone near 50-55 km (Randall et al., 2017). However, when the satellite is in a higher orbit, these perturbations can generally be disregarded for the detection signals. Previous studies on AIM satellite's detection of PMCs have also not focused extensively on this issue.

We added some description to Section 2.1 (lines 87 to 110). The added parts after the revision are highlighted in red italics.

“... Similar to the CIPS, the WFUI was designed as a nadir camera to image sunlight scattering signals by ice particles of PMCs in the 265 nm UV band. Figure 1a demonstrates the reason for using the 265 nm UV band for WFUI. The designated band of UV radiation from the sun in space first reaches the PMCs and is scattered by the ice particles of the PMCs with a radius of 5–100 nm. The scattered light within the FOV of the WFUI was received and imaged. The calculation results obtained from the Line-By-Line Radiative Transfer Model (LBLRTM) software, shown in Fig. 1b, indicate that the atmospheric transmittance of solar radiation with wavelengths of 265 nm above 70 km was close to 1. This implies that the radiation can almost reach the PMCs without significant loss.

The satellite data indicates that total ozone varies strongly with latitude over the globe, with the largest values occurring at middle and high latitudes during most of the year. In the Antarctic, a pronounced minimum in total ozone is observed during spring. Typical values vary between 200 and 500 Dobson units (DU) over the globe, with a global average abundance of about 300 DU (Salawitch et al., 2023). In Figs.1b to 1d, our calculations by using LBLRTM show that even lower concentrations of ozone can effectively absorb solar UV radiation. This prevents UV radiation from below altitudes of 40 km, which is scattered by the ground, lower

atmosphere, and cloud/aerosol layer, from being uploaded, ensuring that it does not interfere with the detection signal at the PMCs altitude. The curve in Fig. 1c demonstrates strong absorption of the atmosphere below 70 km with wavelengths of 265 nm. This absorption is primarily attributed to the distribution of ozone in the stratosphere at altitudes ranging from 20 to 40 km, with a peak concentration occurring at altitudes ranging from 20 to 25 km (the distribution of ozone transmission with altitude is shown in Fig. 1d).

In addition, the scattering of UV radiation by atmospheric molecules from 40 to 80 km causes weak interference in the detection of PMCs. Studies have found that after the AIM satellite's orbit was lowered, it could detect Rayleigh scattering of 265 nm radiation at altitudes around 50-55 km when there were no PMCs. The perturbations to the observed Rayleigh scattering signal on scales of tens to hundreds of kilometers generally indicate GW-induced variations in the neutral density and/or ozone near 50-55 km (Randall et al., 2017). However, when the satellite is in a higher orbit, these perturbations can generally be disregarded for the detection signals. Previous studies on AIM satellite's detection of PMCs have also not focused extensively on this issue. ...”

We have added two references to the end:

“Randall, C. E., Carstens, J., France, J.A., Harvey, V. L., Hoffmann, L., Bailey, S.M., Alexander, M. J., Lumpe, J.D., Yue, J., Thurairajah, B., Siskind, D. E., Zhao, Y., Taylor, M.J., Russell, J.M.: New AIM/CIPS global observations of gravity waves near 50–55 km, Geophys. Res. Lett., 44(13), 7044–7052, <https://doi.org/10.1002/2017GL073943>, 2017.”

“Salawitch, R. J., McBride, L. A., Thompson, C. R., Fleming, E. L., McKenzie, R. L., Rosenlof, K. H., Doherty, S. J., Fahey, D. W.,: Twenty Questions and Answers About the Ozone Layer: 2022 Update, Scientific Assessment of Ozone Depletion: 2022, 75, <https://csl.noaa.gov/assessments/ozone/2022>, 2023.”

6. Page 18, lines 420-423: This analysis and the results shown in Figure 8 (panels (b), (e), (f)) suggest that WFUI would be less effective in observing the early and late portions of a typical PMC season, as well as latitudes equatorward of 65 degrees.

Thanks for pointing this out. We appreciate for your analysis, and we have added this analysis into this paragraph (lines 438-440) as:

“... From Fig. 9, there is a strong correlation between the IWC of the PMCs and the detection efficiency, with the numerical distribution following an exponential function pattern. When the IWC was relatively low, the detection efficiency increased rapidly as the IWC increased. However, once the IWC reached a higher level, the rate of increase in the detection efficiency decreased with further increments in the IWC. This analysis and the results shown in Figure 8 (panels (b), (e), (f)) suggest that WFUI would be less effective in observing the early and late portions of a typical PMCs season, as well as latitudes equatorward of 65 ° ...”

7. Page 20, lines 454-458: These results indicate that changing instrument parameters doesn't improve the detection efficiency at the start or end of a PMC season. Did you evaluate these options at different latitudes?

Thank you for pointing this out. We are also very interested in this issue. Consequently, we conducted a further parameter sensitivity analysis on detection efficiency at different latitudes during various periods of the PMCs season. We have also updated the title of section 4.4 to

“Parameter Sensitivity Analysis and Discussion”. The results are shown in the figure below.

We added some description to Section 4.4 (lines 483 to 491) as:

“... The distribution of PMCs exhibits a strong latitude dependency. To further investigate the impact of parameter changes on detection efficiency at different latitudes, we conducted a sensitivity analysis of detection efficiency for PMCs across various latitudes and seasonal periods. Specifically, we divided the latitude range from 55 ° to 85 ° into 5 ° intervals and analyzed the detection efficiency of PMCs during various periods using the same orbit and parameters. The results are shown in Figure 11. Figure 11 shows that during the early and late stages of PMCs season, parameter changes have minimal impact on detection efficiency across different latitudes. During the early stage of the PMCs season, the appearance of PMCs is infrequent and faint, resulting in a detection efficiency of less than 10% during this period. However, during the early-mid, mid, and mid-late stages of the PMCs season, parameter changes significantly affect detection efficiency in the latitude range of 65 ° to 85 °, while the impact is relatively limited in the latitude range of 55 ° to 65 °”

The added Figure 11 and the captions are shown as follows:

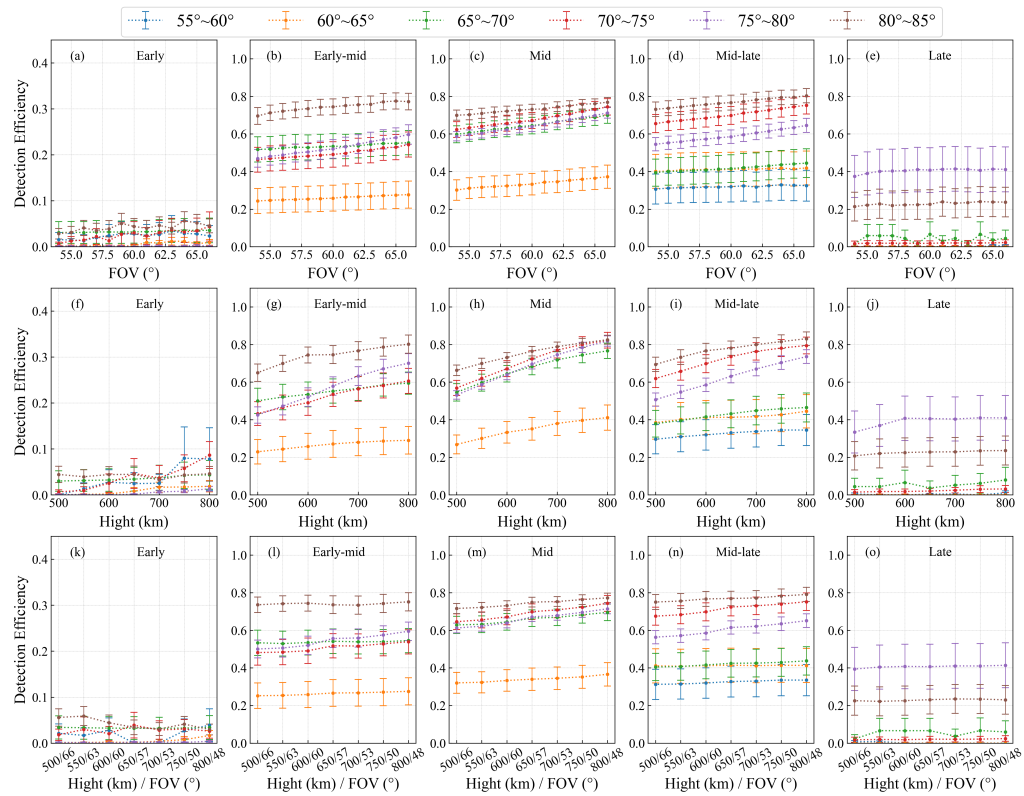


Figure 11: (a)-(e) Variation in detection efficiency with the FOV at different latitudes during different periods; (f)-(j) Variation in detection efficiency with the satellite altitude at different latitudes during different periods; (k)-(o) variation in detection efficiency with simultaneous changes in the FOV and satellite altitude at different latitudes during different periods.

Special thanks to the reviewer for his/her good comments.

We have tried our best to revise and improve the manuscript and made a few changes in the manuscript according to the reviewer's good comments. Again, many thanks for your valuable comments and suggestions. We would like to have our paper at your disposal.

We appreciate for reviewer's spending more time on reviewing over paper and offering valuable suggestions and hope that the modification and corrections will meet with approval and hoping that our paper will be published in *Atmospheric Measurement Techniques* as soon as possible.

We look forward to your information about my revised paper.

Yours sincerely,
Ke Ren and Haiyang Gao